agronomy

MDPI

*Article*

# Biochar Amendment as a Mitigation Against Freezing–Thawing Effects on Soil Hydraulic Properties

**Zhongkui Chen [1], Chitipat Intraravimonmata [2], Viroon Kamchoom [2,*], Rui Chen [3] and Natdanai Sinsamutpadung [2]**

[1] Shenzhen Yanzhi Science and Technology Co., Ltd., Shenzhen 518101, China; brucechenyzte@163.com
[2] Excellent Centre for Green and Sustainable Infrastructure, School of Engineering, King Mongkut's Institute of Technology Ladkrabang, Bangkok 10520, Thailand; 62601007@kmitl.ac.th (C.I.); natdanai.si@kmitl.ac.th (N.S.)
[3] School of Civil and Environmental Engineering, Harbin Institute of Technology Shenzhen, Shenzhen 518055, China; cechenrui@hit.edu.cn
* Correspondence: viroon.ka@kmitl.ac.th

**Abstract:** Seasonal freeze–thaw cycles compromise soil structure, thereby increasing hydraulic conductivity but diminishing water retention capacity—both of which are essential for sustaining crop health and nutrient retention in agricultural soils. Prior research has suggested that biochar may alleviate these detrimental effects; however; further investigation into its influence on soil hydraulic properties through freeze–thaw cycles is essential. This study explores the impact of freeze–thaw cycles on the soil water retention and hydraulic conductivity and evaluates the potential of peanut shell biochar to mitigate these effects. Peanut shell biochar was used, and its effects on soil water retention and unsaturated hydraulic conductivity were evaluated through evaporation tests. The findings indicate that freeze–thaw cycles predominantly affect clay's ability to retain water and control hydraulic conductivity by generating macropores and fissures; with a notable increase in conductivity at high matric potentials. The impact lessens as matric potential decreases below −30 kPa, resulting in smaller differences in conductivity. Introducing biochar helps mitigate these effects by converting large pores into smaller micro- or meso-pores, effectively increasing water retention, especially at higher content of biochar. While biochar's impact is more pronounced at higher matric potentials, it also significantly reduces conductivity at lower potentials. The total porosity of the soil increased under low biochar application rates (0% and 1%) but declined at higher application rates (2% and 3%) as the number of freeze–thaw cycles increased. Furthermore, the characteristics of soil deformation during freeze–thaw cycles shifted from frost heaving to thaw settlement with increasing biochar application rates. Notably, an optimal biochar application rate was observed to mitigate soil deformation induced by freeze–thaw processes. These findings contribute to the scientific understanding necessary for the development and management of sustainable agricultural soil systems.

**Keywords:** freezing–thawing; peanut shell biochar; compaction; soil water retention curve; unsaturated hydraulic conductivity



Academic Editor: Huashou Li

Received: 22 November 2024
Revised: 30 December 2024
Accepted: 6 January 2025
Published: 8 January 2025

**Citation:** Chen, Z.; Intraravimonmata, C.; Kamchoom, V.; Chen, R.; Sinsamutpadung, N. Biochar Amendment as a Mitigation Against Freezing–Thawing Effects on Soil Hydraulic Properties. *Agronomy* **2025**, *15*, 137. https://doi.org/10.3390/agronomy15010137



## 1. Introduction

Water retention and hydraulic conductivity present critical challenges in soil management, especially in regions experiencing seasonal freeze–thaw cycles. In agricultural soils, maintaining adequate moisture levels is essential to crop health, as it supports nutrient retention and provides a stable environment for root systems. However, freeze–thaw cycles weaken soil aggregates, leading to structural breakdown over time [1–3]. This structural

degradation poses challenges in agricultural systems, where it can hinder root development and limit nutrient uptake, both essential for crop resilience. More importantly, the repeated process of freezing and thawing enhances the development of cracks and fissures within the soil matrix [4–6]. Upon freezing, water within the soil expands, exerting considerable pressure on the soil matrix that alters pore structures and disrupts the natural movement of water and air within unsaturated soils [7–11]. This process may lead to the formation of larger pores that enhance hydraulic conductivity; however, it concurrently reduces the soil's water retention capacity [12–14], a critical factor for sustaining plant growth in agricultural environments.

The use of nature-based solutions has garnered interest, particularly with respect to biochar [15,16]. This material, derived from biomass pyrolysis, is noted for its porosity, high carbon content, and substantial adsorption capacity, which have led to extensive investigations in geo-environmental engineering [17–22]. Studies have explored its efficacy in mitigating the negative impacts of cyclic freezing and thawing. Faloye et al. [23] showed that biochar improved soil hydro-physical properties, which significantly enhanced water retention and maize yield, especially when combined with irrigation and fertiliser. Faloye et al. [24] also demonstrated that biochar can improve water retention and efficiency in maize cultivation, enabling a 40% reduction in irrigation needs while maintaining high grain yield. Jabro et al. [25] and Hussain et al. [26] found that biochar's porosity allows for increased air and water permeability within the soil matrix, which can help maintain soil structure even as the soil undergoes repeated freeze–thaw cycles. Biochar may offer a strategic benefit in cold-climate agriculture by improving soil moisture availability and reducing crop stress. However, replicating these results in the field is challenging due to variability in soil density, compaction, water content, and temperature. This variability might limit the extent to which biochar can maintain soil structure and improve water retention capacity. Therefore, gaining a comprehensive understanding of the unsaturated hydraulic properties of biochar-amended soils is crucial for the effective utilisation of biochar in cold regions.

The objectives of this study are (i) to explore the influence of cyclic freezing–thawing on the unsaturated hydraulic properties of biochar-amended clay (BAC) with varying biochar contents and compaction water contents, and (ii) to comprehend the impact of soil compaction (i.e., soil dry density) on the $K_s$ of the BAC subjected to freezing–thawing cycles. For this purpose, a series of evaporation tests were carried out on the compacted clay with peanut shell biochar. The soil water retention curve (SWRC) and unsaturated hydraulic conductivity of BAC with different biochar contents were measured. Moreover, the $K_s$ of BAC was quantified through falling head tests. The measured results among different test groups were compared and analysed. The novelty of the study lies in its investigation of the unsaturated hydraulic properties of biochar-amended clay under various cycles of freezing–thawing. This is an important contribution to the field of soil science, as it provides valuable insight into the behaviour of biochar in cold and dry areas, which can help to improve the function of biochar-amended agriculture soils and reduce soil water loss. The findings of this study can thus provide a reference for optimising biochar content and compaction techniques for agricultural fields, where improved soil structure and moisture retention are key to sustaining crop productivity in cold climates.

## 2. Materials and Methods

### *2.1. Test Programme*

This study involved extensive laboratory experiments aimed at investigating the effects of freezing–thawing cycles, biochar content, compaction water content, and soil dry density on the hydraulic properties. To achieve this, a total of 68 samples were prepared, each with a different combination of the four aforementioned factors. Specifically, four different cycles of

the freezing–thawing process (0, 1, 3, 8, and 12), four levels of biochar content (0%, 2%, 4%, and 8%), three levels of compaction water content (30%, 34%, and 38%), and three levels of soil dry density (1.105, 1.170, and 1.235 g $cm^{-3}$) were utilised. A control group, consisting of soil without any biochar amendment, was established with a soil dry density of 1.170 g $cm^{-3}$ and a compaction water content of 34%. The details of all the tests conducted in this study are summarised in Table 1.

**Table 1.** Test summary.

| Test ID | Cycles of Freezing–Thawing (Cycles) | Biochar Content (%) | Compaction Water Content (%) | Soil Dry Density (g $cm^{-3}$) | Soil Hydraulic Property | | Microstructure Observation | |
|---|---|---|---|---|---|---|---|---|
| | | | | | $K_s$ | SWRC | SEM | MIP |
| N0B0 | 0 | 0 | 34 | 1.105 | √ | | | |
| | | | | 1.170 | √ | | | |
| | | | | | √ | √ | √ | √ |
| | | | 30 | 1.235 | | √ | | |
| | | | 38 | | | √ | | |
| N0B2 | | 2 | 34 | 1.105 | √ | | | |
| | | | | 1.170 | √ | | | |
| | | | | 1.235 | √ | | | |
| N0B4 | | 4 | 34 | 1.105 | √ | | | |
| | | | | 1.170 | √ | | | |
| | | | | 1.235 | √ | | | |
| N0B8 | | 8 | 34 | 1.105 | √ | | | |
| | | | | 1.170 | √ | | | |
| | | | | | √ | √ | √ | √ |
| | | | 30 | 1.235 | | √ | | |
| | | | 38 | | | √ | | |
| N1B0 | 1 | 0 | 34 | 1.105 | √ | | | |
| | | | | 1.170 | √ | | | |
| | | | | 1.235 | √ | | | |
| N1B2 | | 2 | 34 | 1.105 | √ | | | |
| | | | | 1.170 | √ | | | |
| | | | | 1.235 | √ | | | |
| N1B4 | | 4 | 34 | 1.105 | √ | | | |
| | | | | 1.170 | √ | | | |
| | | | | 1.235 | √ | | | |
| N1B8 | | 8 | 34 | 1.105 | √ | | | |
| | | | | 1.170 | √ | | | |
| | | | | 1.235 | √ | | | |
| N3B0 | 3 | 0 | 34 | 1.105 | √ | | | |
| | | | | 1.170 | √ | | | |
| | | | | 1.235 | √ | | | |
| N3B2 | | 2 | 34 | 1.105 | √ | | | |
| | | | | 1.170 | √ | | | |
| | | | | 1.235 | √ | | | |
| N3B4 | | 4 | 34 | 1.105 | √ | | | |
| | | | | 1.170 | √ | | | |
| | | | | 1.235 | √ | | | |
| N3B8 | | 8 | 34 | 1.105 | √ | | | |
| | | | | 1.170 | √ | | | |
| | | | | 1.235 | √ | | | |

**Table 1.** *Cont.*

| Test ID | Cycles of Freezing–Thawing (Cycles) | Biochar Content (%) | Compaction Water Content (%) | Soil Dry Density (g cm$^{-3}$) | Soil Hydraulic Property | | Microstructure Observation | |
|---|---|---|---|---|---|---|---|---|
| | | | | | $K_s$ | SWRC | SEM | MIP |
| N8B0 | 8 | 0 | 34 | 1.105 | √ | | | |
| | | | | 1.170 | √ | | | |
| | | | | 1.235 | √ | | | |
| N8B2 | | 2 | 34 | 1.105 | √ | | | |
| | | | | 1.170 | √ | | | |
| | | | | 1.235 | √ | | | |
| N8B4 | | 4 | 34 | 1.105 | √ | | | |
| | | | | 1.170 | √ | | | |
| | | | | 1.235 | √ | | | |
| N8B8 | | 8 | 34 | 1.105 | √ | | | |
| | | | | 1.170 | √ | | | |
| | | | | 1.235 | √ | | | |
| N12B0 | 12 | 0 | 34 | 1.105 | √ | | | |
| | | | | 1.170 | √ | | | |
| | | | | | √ | √ | √ | √ |
| | | | 30 | 1.235 | | √ | | |
| | | | 38 | | | √ | | |
| N12B2 | | 2 | 34 | 1.105 | √ | | | |
| | | | | 1.170 | √ | | | |
| | | | | 1.235 | √ | | | |
| N12B4 | | 4 | 34 | 1.105 | √ | | | |
| | | | | 1.170 | √ | | | |
| | | | | 1.235 | √ | | | |
| N12B8 | | 8 | 34 | 1.105 | √ | | | |
| | | | | 1.170 | √ | | | |
| | | | | | √ | √ | √ | √ |
| | | | 30 | 1.235 | | √ | | |
| | | | 38 | | | √ | | |

The selection of factors in this study was based on their potential to impact the hydraulic properties of BAC. To determine the appropriate levels for each factor, prior research studies and practical considerations were taken into account. Freezing–thawing cycles, for example, can cause changes in soil structure that significantly affect the unsaturated hydraulic properties of soil. Therefore, this factor was included at different levels based on the relevant range of soil structure changes induced by freezing and thawing. Preliminary experiments showed that 12 cycles were sufficient to capture the extent of soil structure changes in bare soil induced by freezing–thawing cycles. Biochar content was included due to its potential to improve soil water retention and decrease hydraulic conductivity. The levels of biochar content were chosen based on the commonly used range of values in BAC research, beyond which further biochar addition may not yield significant improvements in soil hydraulic properties [27]. Compaction water content was also considered due to its ability to influence soil density and porosity, ultimately affecting soil hydraulic properties. The compaction water content levels were selected based on the soil water content range under field conditions, which is approximately 4% dry and 4% wet of the optimum water content. Lastly, soil dry density was included because it can impact soil structure and, consequently, affect its hydraulic properties. The levels of soil dry density were chosen based on common values for loosely, moderately, and densely compacted soil. The findings from this study provide essential insights into optimising BAC for its intended use, such as reducing soil water loss in cold and dry areas.

### 2.2. Sample Preparation

Figure 1 represents the compacted clay amended with biochar used in this study. The biochar was acquired from a recycled material company located in China. It was derived from agricultural waste material, specifically peanut shells, through the process of slow pyrolysis. The pyrolysis was carried out under anaerobic conditions at a temperature of 500 °C for one hour. The biochar derived from peanut shells exhibits a honeycomb-like microstructure, with a specific gravity of 2.07 and a small pore volume, while presenting a large surface area [17]. To remove any impurities and peanut shell debris that had not undergone complete pyrolysis and had a diameter larger than 0.5 mm, a sieve was utilised prior to clay amendment use. Furthermore, to eliminate the impact of original moisture content, all biochars utilised in the experiments were subjected to oven drying at 105 °C for 24 h. The clay used in the experiment was commercial kaolin clay, with basic physical properties determined in accordance with the test standard GB/T 50123-2019 [28]. The basic properties of the clay were reported in Ng et al. [29]. According to the Unified Soil Classification System (USCS), the kaolin clay used in this study has a liquid limit of 78.5% and a plasticity index of 46.9%, classifying it as a high-plasticity clay (CH). Dry clay powder was mixed with dry biochar at prescribed application rates. Subsequently, the mixture was combined with water to reach the targeted gravimetric water content of 30%, 34%, and 38%, representing the dry optimum, optimum, and wet optimum water contents of the clay, respectively. The resulting moist BAC mixture was allowed to equilibrate in a sealed plastic bag for 24 h. Finally, the BAC mixture was compacted in a customised stainless-steel cylinder that had an inner diameter of 65 mm and a height of 95 mm as shown in Figure 1.

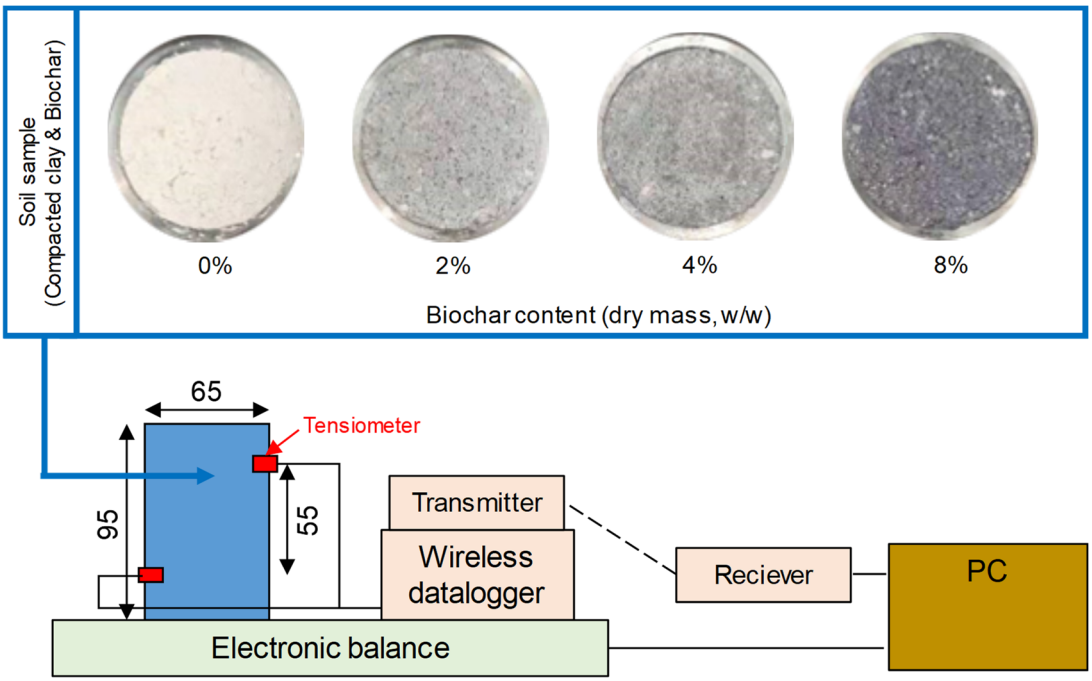


**Figure 1.** Schematic representation of compacted clay amended with biochar, depicting different biochar contents (B0, B2, B4, B8 denote 0%, 2%, 4%, and 8% biochar content, respectively), unit: mm.

### 2.3. The Simulation of Freezing–Thawing Cycles

Following the compaction of soil samples in cylinders, the soil samples and cylinder were moved to a temperature and humidity control chamber (CK-800G model; Dongguan Qinzhuo Environmental Testing Equipment Co., Ltd, Dongguan, Guangdong, China) to simulate controlled freezing–thawing cycles. The purpose was to investigate the impact of freezing–thawing cycles, biochar content, compaction water content, and soil dry density

on the hydraulic properties of BAC. To prevent moisture loss from the samples to the air in the test chamber, each cylinder was wrapped with a plastic film, which allowed the water or vapour in the soil samples to not interact with the outer environment during the entire freezing–thawing process. The freezing–thawing process was conducted in compliance with the ASTM standard [30]. The temperature range controlled by the chamber was between −60 °C and 150 °C with an accuracy of ±0.1 °C, and a freezing temperature of −15 °C and a thawing temperature of 20 °C were chosen to simulate environmental conditions representative of the range experienced in the field, particularly in the winter of northeast China. The soil samples were subjected to 0, 1, 3, 8, and 12 freezing–thawing cycles, and upon completion of the designated cycle number, they were removed from the chamber and tested for hydraulic conductivity, micro-structure analysis of mercury intrusion porosimetry (MIP), and scanning electron microscopy (SEM).

### *2.4. Measurement of Saturated Water Hydraulic Conductivity of BAC*

The measurement of the $K_s$ of the BAC was conducted using the falling head method, which is in accordance with the standard GB/T 50123-2019. To perform the falling head tests, a permeameter (Model TST-55) was used. A filter paper was placed at the top and bottom of each soil specimen, and a porous stone was placed on the filter paper at each end. To saturate the samples, the vacuum saturation method, as described in ASTM C1202-2006 [31], was employed. In this method, the sample was initially placed in a vacuum container for 3 h without water, followed by introducing de-aerated water into the container until all the samples were submerged for 8 h.

### *2.5. Measurement of Soil Water Retention Curve and Unsaturated Hydraulic Conductivity*

In this study, a simplified evaporation test method was employed to measure the SWRC and hydraulic conductivity function. This method was preferred due to its two notable advantages: (i) it requires a shorter testing duration, and (ii) it allows for the simultaneous measurement of SWRC and unsaturated hydraulic conductivity, as reported by Schindler et al. [32]. SWRC is a crucial parameter that characterises the relationship between soil moisture content and matric potential. The evaporation test was used to determine the drying curve of the SWRC. The evaporation tests involved the measurement of soil matric potential and water content using a combination of tensiometers and an electronic balance. The experimental setup for conducting evaporation test is illustrated in Figure 1. In this setup, the SWRC and unsaturated hydraulic conductivity can be simultaneously obtained [33]. The kaolin clay was mixed with peanut shell biochar and water was added to attain the optimum water content of the BAC mixture. Peanut shell biochar was chosen due to its unique properties, including its smaller average pore diameter (3.72 nm), and larger specific surface area (43.5 $m^2/g$), which are suitable for enhancing soil water retention. Customised stainless-steel columns with an inner diameter of 65 mm, an outer diameter of 70 mm, and a height of 95 mm were used to compact soil samples. Each soil sample was compacted into five sub-layers, and the soil surface between consecutive sub-layers was carefully scratched to achieve good contact between the two sub-layers. The BAC was compacted to reach the target dry density, which corresponds to 1.235 g $cm^{-3}$. The soil samples were saturated by placing them in a vacuum chamber following the ASTM C1202 standard [31]. After compaction, the soil cylinder was sealed at the bottom, and two holes were drilled on the side of the soil sample at a vertical spacing of 55 mm between the holes.

The evaporation test was conducted in a laboratory under relatively constant temperature and humidity conditions. High-capacity tensiometers (Model YZ-500; Shenzhen Yanzhi Science and Technology Co., Ltd, Shenzhen, Guangdong, China) were installed in each hole to capture the variation in soil matric potential to cover a wider range of pore

water pressure (PWP). The tensiometer can measure matric potential directly from 0 to −500 kPa with an accuracy of 2 kPa [34]. The readings of the upper and lower tensiometers and the water loss changes in soil samples were automatically collected in real-time by the wireless data logger and the electronic balance, respectively. The average matric potential value of the two tensiometer readings was used to form the SWRC. The measured SWRC was fitted using the Van Genuchten (VG) model [35] (see Equation (1)). Furthermore, the unsaturated hydraulic conductivity function of the BAC was obtained following Equations (2) and (3).

$$\theta = \theta_r + \frac{(\theta_s - \theta_r)}{[1 + (\alpha\psi)^n]^m} \quad (1)$$

$$k(\overline{\psi}) = \frac{\Delta V}{2A \cdot \Delta t \cdot i_m} \quad (2)$$

$$i_m = \frac{1}{2}\left(\frac{\psi_{t1,upper} - \psi_{t1,lower}}{\Delta z} + \frac{\psi_{t2,upper} - \psi_{t2,lower}}{\Delta z}\right) - 1 \quad (3)$$

where $\theta$ is the volumetric water content (%); $\psi$ is the soil matric potential; $\theta_r$ and $\theta_s$ are the residual and saturated volumetric water content; $\alpha$ is an empirical scale parameter; $n$ is the curve shape factor which controls the slope of the SWRC; and $m$ is an empirical shape factor related to $n$ by $m = 1 - 1/n$. $k(\overline{\psi})$ denotes the unsaturated hydraulic conductivity function of the BAC; $\overline{\psi}$ denotes the average matric potential measured by the upper and lower tensiometer, kPa; $\Delta V$ is the volume of water loss in the soil sample during the time $\Delta t$ (30 min in this study), $m^3$; $A$ is the cross-sectional area of the soil sample, $m^2$; $i_m$ is the average hydraulic gradient; $\Delta z$ is the vertical distance between the upper and lower tensiometer, m; $\psi_{t,upper}$ denotes the matric potential measured by the upper tensiometer, kPa; and $\psi_{t,lower}$ denotes the matric potential measured by the lower tensiometer, kPa.

### *2.6. Microstructure Observation*

Following the target freezing–thawing cycles, four soil samples (i.e., B0N0, B8N0, B0N12, B8N12) were taken out of the chamber and trimmed to extract small cubes of approximately 10 × 10 × 10 $mm^3$ from the middle part of the samples. Prior to the SEM and MIP tests, the subsample cubes were pretreated in liquid nitrogen at −195 °C for 5 min and then placed in a vacuum freeze-dryer (−40 °C) for 48 h. Finally, an open-source software, ImageJ v1.8.0 [36], was used to analyse and interpret the SEM images for quantifying the dimension of BAC pores and any micro-crack width introduced by the freezing–thawing cycles. Meanwhile, the pore size distribution of soil samples can be obtained from the MIP test.

## 3. Results and Discussion

### *3.1. Assessing the Adverse Impact of Freezing–Thawing Cycles on Saturated Hydraulic Conductivity Across Various Soil Densities*

Figure 2 illustrates the variation of $K_s$ of BAC with freezing–thawing cycles at different densities and biochar contents. All the samples were compacted at 34% compaction water content. The results showed that the $K_s$ of BAC can be significantly affected by freeze–thaw cycles. For all three densities, the $K_s$ of bare soils increased with an increase in freezing–thawing cycles. The effect of the first three freeze–thaw cycles is more pronounced than the following cycles. This increase in $K_s$ was in agreement with previous studies [4,7]. During freezing, water in soil pores can expand and exert pressure on the surrounding soil particles, leading to soil heaving and pore collapse. As a result, soil porosity and hydraulic conductivity can be reduced, which can limit water infiltration and increase surface runoff. During thawing, the opposite effect can occur, with the formation of large soil pores, especially those larger than 10 μm (as can be seen from Figure 3), and thus increased hydraulic conductivity. The occurrence of cracks was

also induced by freezing–thawing (as depicted in Figure 4), which created preferential pathways for water flow.

Compared to the dense sample (i.e., 1.235 g $cm^{-3}$), it is expected that the $K_s$ of 1.235 g $cm^{-3}$ was lower than that of the loose and moderately dense samples (i.e., 1.105 g $cm^{-3}$ and 1.170 g $cm^{-3}$, respectively). The compaction can also affect the magnitude of the increase in $K_s$ during freezing–thawing cycles. After cycles of freeze–thaw, the increment of $K_s$ for the dense sample still be lower than that of the low compaction one. For instance, after 12 freeze–thaw cycles, $K_s$ increased from $1.8 \times 10^{-8}$ m/s to $2.7 \times 10^{-7}$ m/s (about 15 times) for the dense sample, which was much less than that from $1.2 \times 10^{-7}$ m/s to $5.4 \times 10^{-6}$ m/s (about 45 times) for the loose sample. The results indicate that with an increase in dry density to 1.235 g $cm^{-3}$, a significant decline in soil macropores was observed, resulting in a corresponding reduction in soil hydraulic conductivity. The reduction in soil macropores is particularly significant, as they are more prone to collapse during freezing–thawing cycles. Thus, minimising the presence of soil macropores becomes crucial in limiting the increase in soil hydraulic conductivity during such cycles.

### *3.2. Mitigation of the Negative Effects of Freezing–Thawing Cycles on the Saturated Hydraulic Conductivity Through Biochar Addition*

The BAC exhibited considerably lower $K_s$ values for all three soil densities examined (Figure 2b–d). For instance, in the case of no freezing–thawing cycles, $K_s$ values decreased from $1.8 \times 10^{-8}$ m/s to $3.8 \times 10^{-9}$ m/s for the dense sample when the biochar content increased from B0 to B8. This may be because when biochar is added to clay soil, the soil particles become more densely packed, leading to a higher proportion of macropores within the soil structure. The larger size of biochar particles relative to soil particles allows them to occupy the spaces between soil particles, thereby leading to a decrease in the number of macropores within the soil.

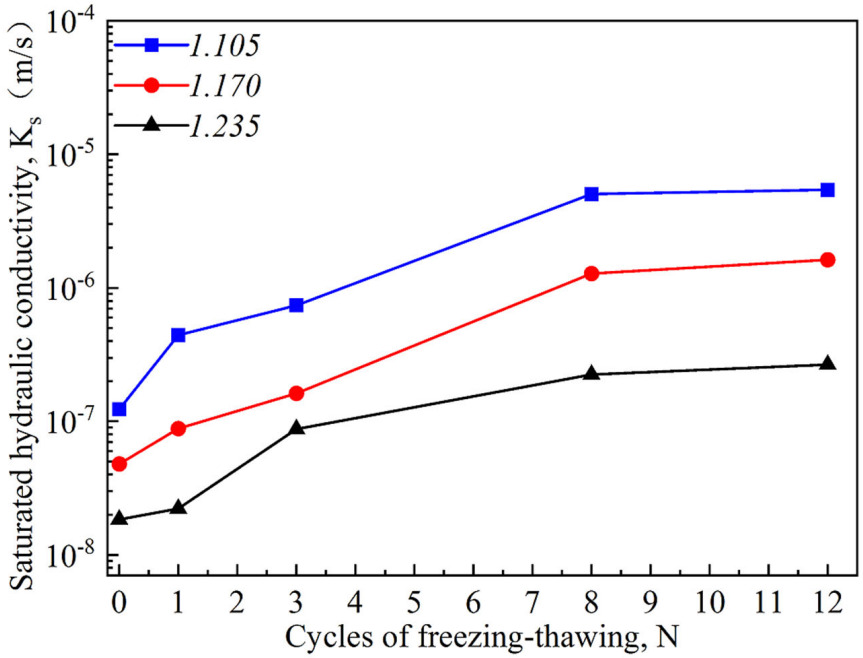


(**a**) B0

**Figure 2.** *Cont.*

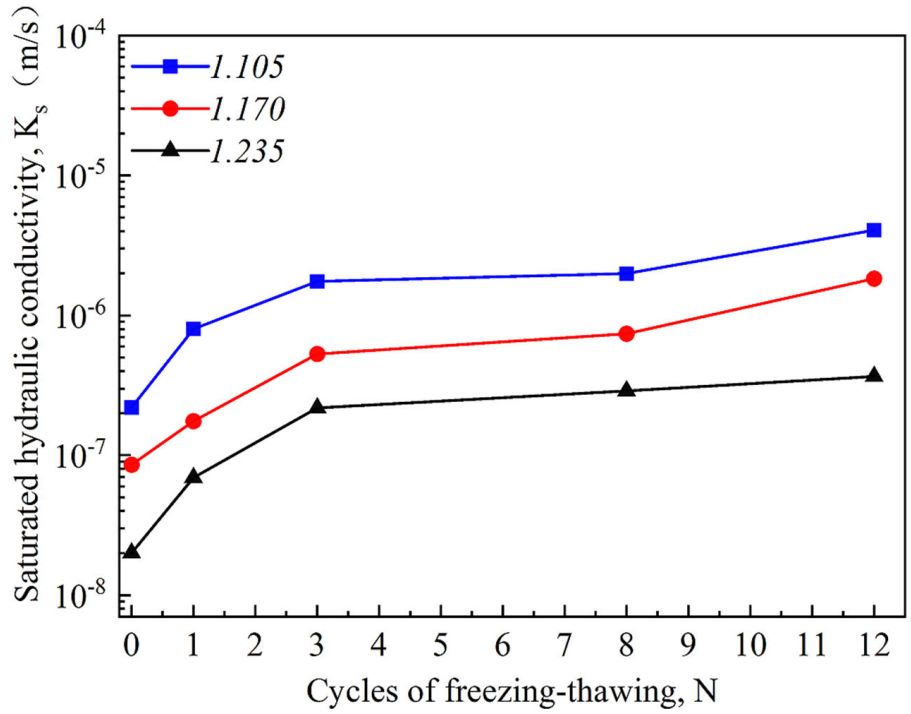


(**b**) B2

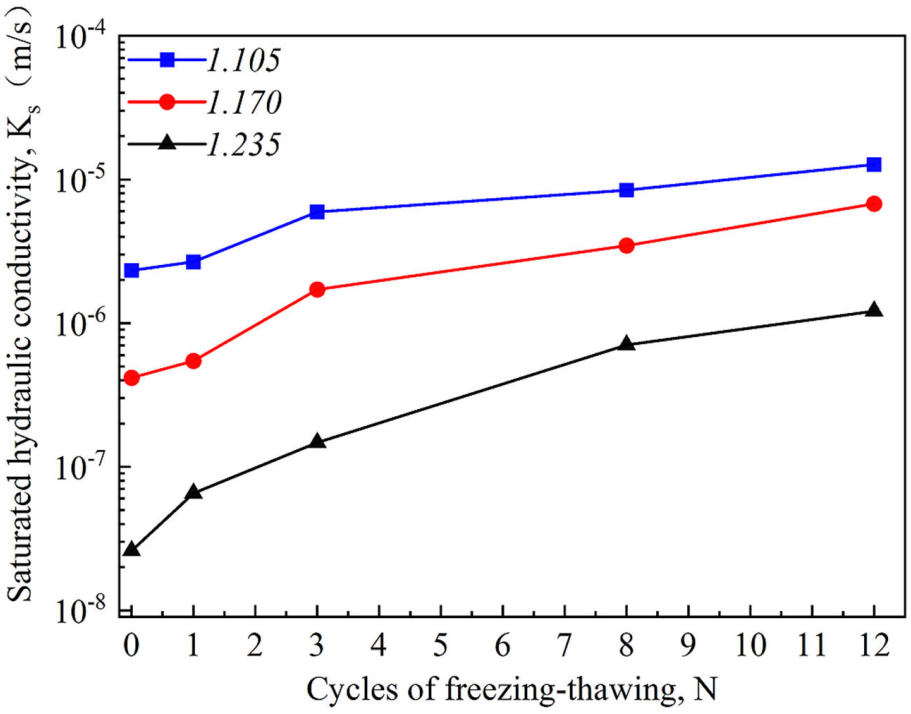


(**c**) B4

**Figure 2.** *Cont*.

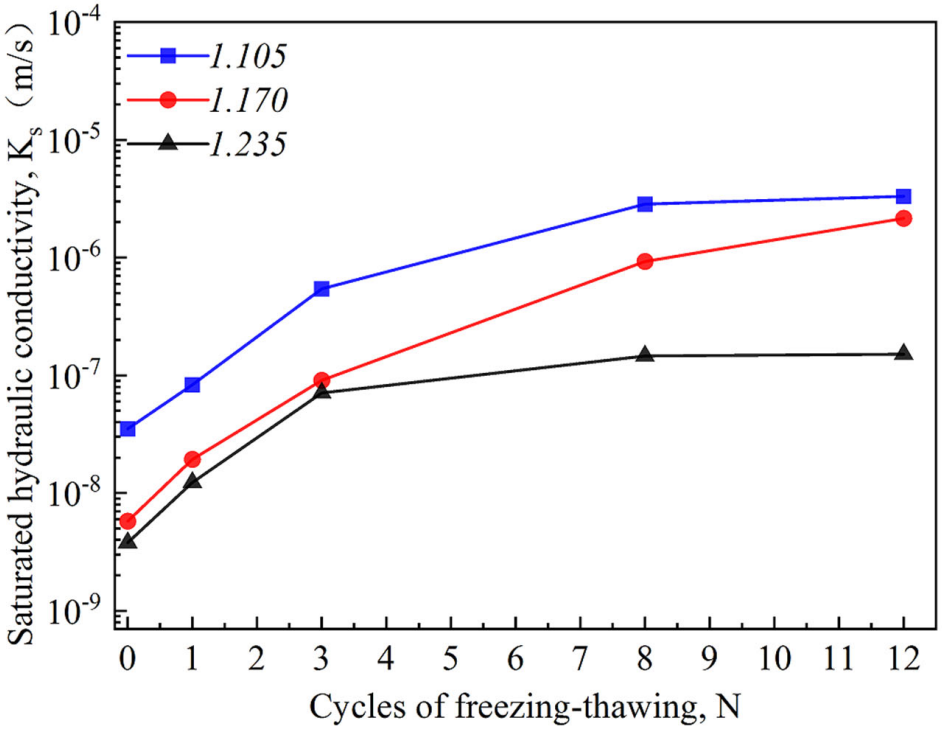


(**d**) B8

**Figure 2.** Variation in soil saturated hydraulic conductivity in response to freezing–thawing cycles and soil densities (1.105 g $cm^{-3}$, 1.170 g $cm^{-3}$, 1.235 g $cm^{-3}$) at different biochar contents: (**a**) 0%, (**b**) 2%, (**c**) 4%, and (**d**) 8%.

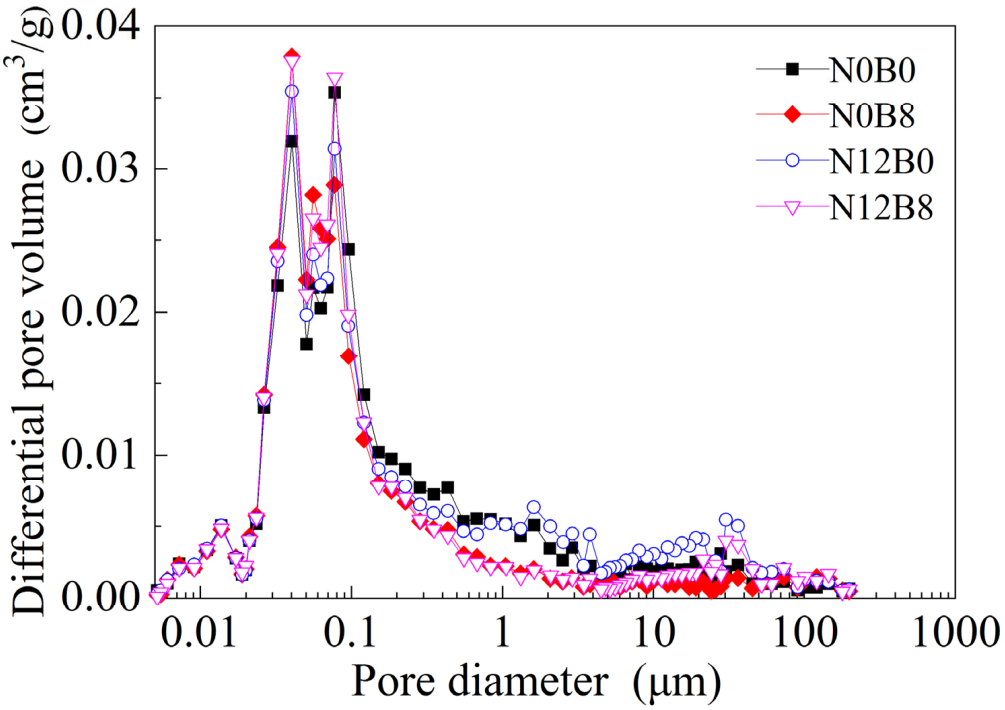


**Figure 3.** Effect of biochar addition on soil microstructure changes caused by freezing–thawing cycles.

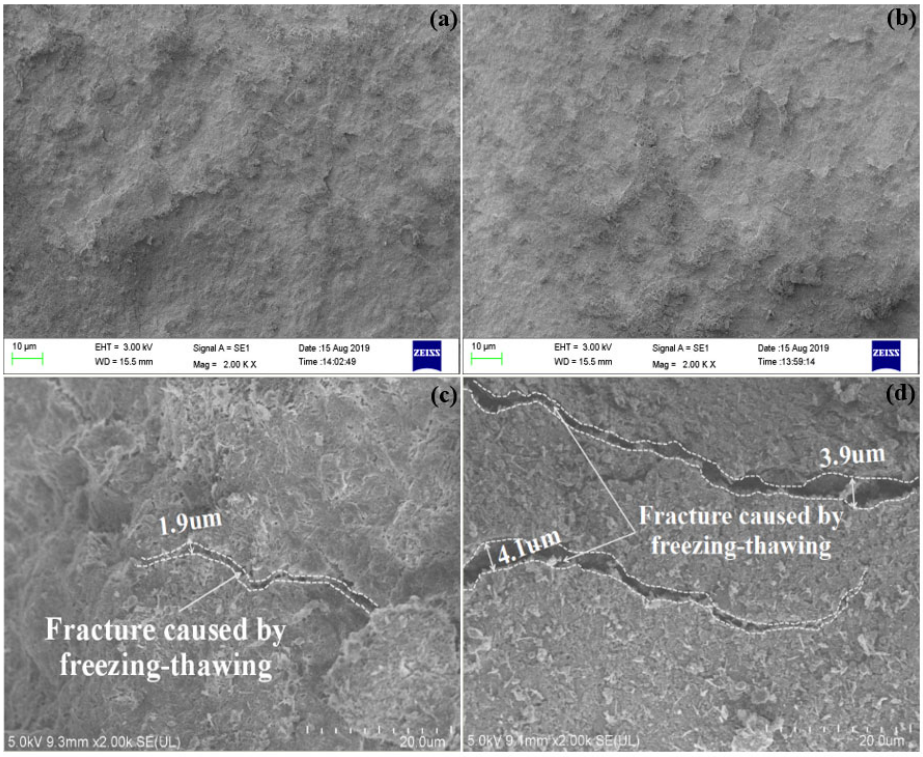


**Figure 4.** SEM image (2000×) of BAC specimens after freezing–thawing cycles: (**a**) B0N0; (**b**) B8N0; (**c**) B0N12; (**d**) B8N12.

Following the cyclic freezing–thawing process, the $K_s$ of all three soil dry densities of BAC increased compared with the case of bare soil. However, their increments for different soil densities are varied. For instance, at a biochar content of 8%, $K_s$ for the lower density (e.g., 1.105 g cm$^{-3}$) increased from 3.5 × 10$^{-8}$ m/s to 3.3 × 10$^{-6}$ m/s (approximately 100 times) after 12 cycles of the freezing–thawing compared to the bare soil. However, when the soil dry density increased to 1.235 g cm$^{-3}$, $K_s$ increased from 3.8 × 10$^{-9}$ m/s to 1.5 × 10$^{-7}$ m/s (approximately 40 times). The difference in the increment of $K_s$ for different soil dry densities may be attributed to the porosity of BAC influencing the transport of water stored in its pores during the freezing–thawing cycles. Generally, soil freezing initiates from the soil surface to the internal pores during the cyclic freezing–thawing process of BAC. In the case of a looser sample, the soil pores are relatively large, making water in the large soil pores easily transportable until it is fully frozen. Therefore, this process of water transport in the large soil pores from the unfrozen area to the frozen area governs the $K_s$. However, for BAC with high density, small pores limit water transport during freezing–thawing. Therefore, the increase in $K_s$ is limited for BAC with higher density and high biochar content (i.e., 8%). This finding suggests that both soil compaction and biochar addition can counteract the effect of cyclic freezing–thawing, especially with high biochar content (i.e., 8%). Moreover, this could be another reason for the reduction of $K_s$ with the increment of BAC due to freezing–thawing cycles. Kumari et al. [37] reported that biochar increased water-dispersible colloid content in amended soils. Dispersed clay colloids may plug or restrict the pores and channels in the soil matrix, leading to altered soil structure and functions [38], such as increased soil compaction and reduced hydraulic conductivity. On the other hand, biochar also contains a large amount of colloidal particles [39]. Freezing–thawing may break the large biochar particles into colloidal particles (Figure 3) and hence reduce the increment of $K_s$. Thus, the application of biochar in clay soil needs to be carefully designed to benefit soil water management in frequently cycled frozen areas.

### *3.3. Improvement of Water Retention in BAC Subjected to Freezing–Thawing Cycles*

The measured SWRC (drainage curves) of BAC under different freezing–thawing cycles is presented in Figure 5. In this figure, N0 and N12 denote 0 and 12 freezing–thawing cycles, while B0 and B8 represent 0% and 8% of biochar content, respectively. The compaction water content is 34% for this figure. The SWRC was fitted using the VG model, and the fitting parameters are summarised in Table 2. The figure illustrates that the addition of 8% biochar significantly improves the water-holding capacity of the soil, regardless of freezing–thawing cycles. As anticipated, the volumetric water content of all soil samples decreased as the soil matric potential decreased. At near saturation, the difference in SWRC between the four groups is minimal. However, as the matric potential decreased, the difference between the groups widened, particularly at low matric potential (lower than −33 kPa, corresponding to the soil matric potential at the field capacity). Biochar affects the water-holding capacity of the soil in the frozen area in two ways. Firstly, the addition of biochar alters the pore size distribution and porosity of the soil, indirectly enhancing the soil water-holding capacity. Secondly, biochar itself possesses porous structures, which can store water in its intra-pores and directly increase the soil water storage capacity. At a specific matric potential beyond the air entry value, the volumetric water content of the soil samples subjected to 12 cycles of freezing–thawing is higher than that of 0 cycles. This implies that cyclic freezing–thawing reduces the soil water-holding capacity. This may be due to the fact that after 12 freeze–thaw cycles, the soil structure could be damaged, as evidenced by the presence of cracks (as shown in Figure 4). These cracks would increase the number of macropores in BAC, consequently increasing water loss under certain soil matric potential. For instance, at the matric potential of −100 kPa, the volumetric water content is 47% and 50% for N12B0 and N12B8, respectively. Moreover, as the biochar content increased from 0% to 8%, the air entry value of BAC increased by 13.3% for N0 and 16.7% after N12.

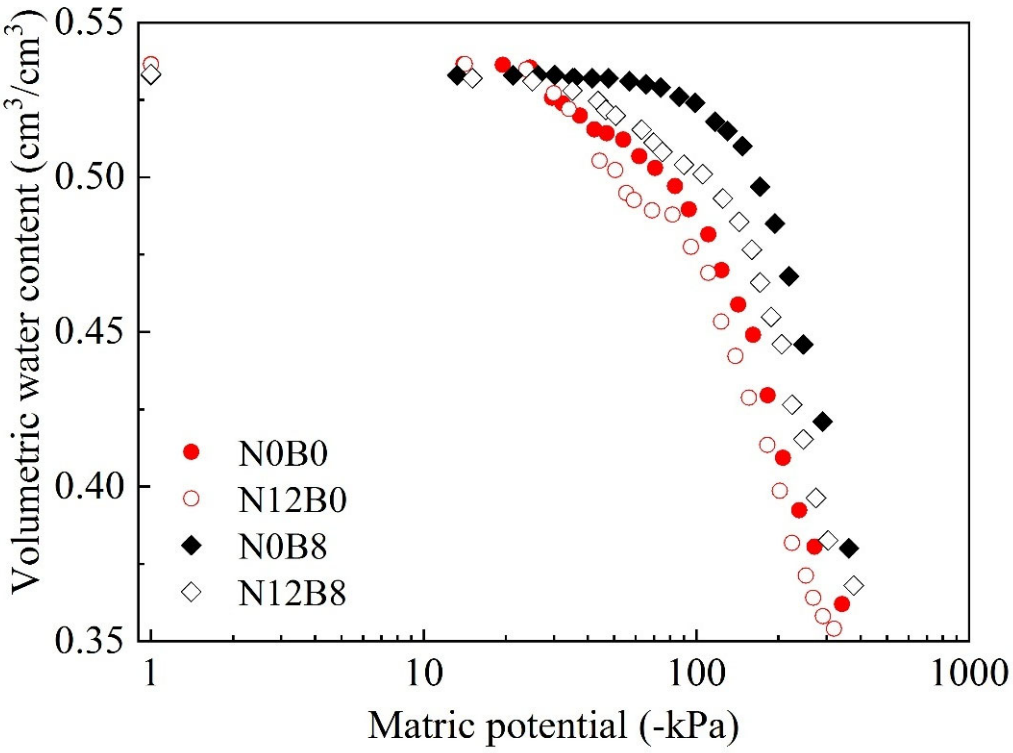


**Figure 5.** Effects of freezing–thawing on the SWRC of BAC with and without biochar treatment.

**Table 2.** Fitting parameters for VG model.

| Test ID | Cycles of Freezing–Thawing (Cycles) | Biochar Content (%) | Compaction Water Content (%) | Soil Dry Density (g cm$^{-3}$) | Fitting Parameters for VG Model | | | | |
|---|---|---|---|---|---|---|---|---|---|
| | | | | | $\theta_S$ | $\alpha$ | $n$ | $m$ | $R^2$ |
| N0B0 | 0 | 0 | 30 | 1.235 | 54.03 | 0.042 | 1.398 | 0.284 | 0.993 |
| | | | 34 | | 53.59 | 0.038 | 1.616 | 0.381 | 0.994 |
| | | | 38 | | 53.45 | 0.033 | 1.705 | 0.414 | 0.995 |
| N0B8 | | 8 | 30 | 1.235 | 53.06 | 0.035 | 2.806 | 0.644 | 0.998 |
| | | | 34 | | 53.26 | 0.033 | 2.014 | 0.503 | 0.999 |
| | | | 38 | | 53.23 | 0.031 | 1.930 | 0.482 | 0.997 |
| N12B0 | 12 | 0 | 30 | 1.235 | 53.90 | 0.050 | 1.672 | 0.402 | 0.995 |
| | | | 34 | | 53.96 | 0.046 | 1.344 | 0.256 | 0.992 |
| | | | 38 | | 53.67 | 0.045 | 1.682 | 0.405 | 0.995 |
| N12B8 | | 8 | 30 | 1.235 | 53.11 | 0.043 | 1.812 | 0.448 | 0.996 |
| | | | 34 | | 52.82 | 0.041 | 2.262 | 0.558 | 0.991 |
| | | | 38 | | 53.05 | 0.037 | 2.114 | 0.527 | 0.996 |

Figure 6 depicts the impact of compaction water content on the soil water retention ability. In this figure, the fitting parameter "$n$" from the VG model was used, which determines the slope of SWRC and the soil water retention ability [33]. The slope of the SWRC becomes steeper as the parameter $n$ increases. As can be seen in the figure, $n$ increases as the compaction water content increases for the control case (N0B0). However, when biochar is added to the clay (N0B8), there is a significant increase in the $n$ value. This clearly demonstrates that biochar addition affects the pore size distribution of BAC. The observed increase in the water retention capacity of clay after the addition of biochar can be attributed to the increase in meso-pores and decrease in macropores, as indicated by the results presented in Figure 3. It is well established that water stored in meso-pores is less prone to drainage and evaporation, making it available for plant uptake [40]. By shifting the pore size distribution towards meso-pores, biochar addition enhances the water retention capacity of the soil, which is in agreement with previous studies [41,42].

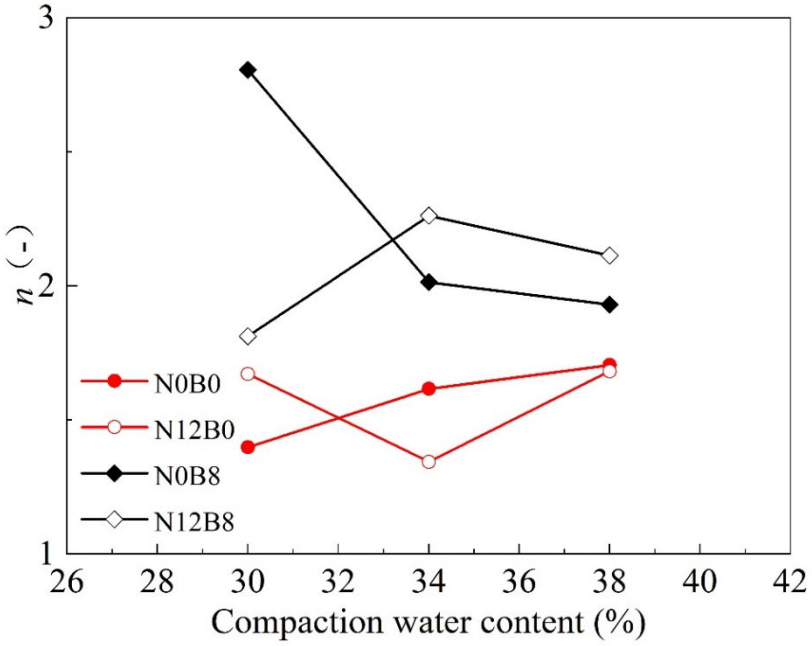


**Figure 6.** The influence of biochar treatment on the water retention properties of compacted BAC at varying compaction water contents and a soil density of 1.235 g cm$^{-3}$.

When subjected to 12 cycles of freezing–thawing (N12B0), the *n* value increases compared to the control case (N0B0) at low compaction water content (i.e., 30%). However, as the compaction water content increased to 34%, the *n* value of soil sample N12B0 becomes lower than that of the control case (N0B0). This is because the freezing–thawing process breaks the large soil particles into small ones and hence mobilises the pore size distribution [43,44] (see Figure 3). The study by Liu et al. [45] revealed that the increase in macroporosity and pore branches could induce the breakdown of macro-aggregates, and Zhang et al. [46] suggested that the soil structure after freeze–thaw cycles changed significantly due to the mechanical fragmentation of soil coarse mineral particles and the aggregation of soil fine particles. Moreover, they concluded that the particle size of soil became more homogeneous and the variation in soil structure weakens as the number of freeze–thaw cycles increased. As the compaction water content increases up to 38%, the *n* value of both soil samples (N0B0 and N12B0) became almost equal, with a difference of only 0.023. This can be explained by the similar distribution of micropores in both soil samples (see Figure 3), as micropores usually dominate the shape of the pore size distribution for soils with high compaction water content.

However, the impact of freezing–thawing on the *n* value changes when the biochar content increases to 8%. At low compaction water content (i.e., 30%), the *n* value of N0B8 is higher than that of N12B8, while the reverse is true as the compaction water content increases. This is because the cyclic freezing–thawing process breaks down the large soil particles into small ones, increasing the content of micropores in the soil samples with high compaction water content. Another possible reason is that the large soil particles break into smaller ones during compaction when the compaction water content is higher. Generally, soil with a higher initial compaction water content provides less void space for soil particles to mobilise during the compaction process [47]. This suggests that it needs to carefully manage the compaction procedure and initial soil water state at the biochar application in frozen areas.

### *3.4. Effects of Freezing–Thawing Cycles on the Unsaturated Hydraulic Conductivity of BAC*

Figure 7 presents the effect of freeze–thaw cycles on the unsaturated hydraulic conductivity of BAC. The results showed that the hydraulic conductivity of BAC significantly increased up to one to two orders of magnitude after subjecting the soil to 12 freeze–thaw cycles, particularly at high matric potential. This may be attributed to the formation of cracks in the soil during the freeze–thaw process, as observed in Figure 3. However, the difference in hydraulic conductivity induced by freeze–thaw cycles decreased when the matric potential exceeded −30 kPa. This was because the water in the soil pores was stored mainly in disconnected micropores or inter-particles of the soil pores in a discontinuous form at low matric potential, and the water in the discontinuous pores was mainly migrated through vapour in the air. This suggests that the impact of freezing–thawing on the soil pore structure was weakened at low matric potential.

Furthermore, the addition of biochar to the soil reduced the hydraulic conductivity of BAC, particularly in the case of N0B8, where the hydraulic conductivity decreased compared to the control case (N0B0). The effect of biochar addition on the reduction in hydraulic conductivity was negligible at low matric potential, but it was significant when BAC was subjected to cyclic freezing–thawing (N12B8) in a wider range of matric potential (Figure 7). This may be because when biochar was added to soil, the fine biochar particles filled the large pores, transforming macropores into micropores or meso-pores (Figure 3). After the BAC was subjected to cyclic freezing–thawing, the soil structure was affected, and more micropores were formed. Moreover, the behaviour of BAC at low matric potential was governed by soil micropores, and adding biochar to clay reduced the

hydraulic conductivity of BAC subjected to cyclic freezing–thawing in a much wider range of matric potential. Zuo et al. [48] conducted indoor simulation experiments on farmland black soil to investigate the effect of biochar addition on freezing–thawing deformation characteristics. They found that biochar application reduced the transformation range and rate induced by the freezing–thawing deformation, significantly increased the soil total porosity, promoted thaw settlement, and restrained frost heaving. Additionally, the soil total porosity increased with low application amounts (0% and 1%) but decreased with high application amounts (2% and 3%) with increasing numbers of freeze–thaw cycles. The characteristics of soil freezing–thawing deformation changed from frost heaving to thaw settlement with increasing biochar application amounts, and an appropriate biochar application amount inhibited soil freezing–thawing deformation. Zhang and Che [49] stated that the modifications of microscopic structure following freeze–thaw could affect the deformation behaviour of soil, and the increase in the average number of cracks (pores) in a unit volume would transform soil displacement from expansion to settlement. However, in this study, the results indicate that 8% biochar content is more effective in counteracting the effect of freezing–thawing to reduce the hydraulic conductivity of BAC.

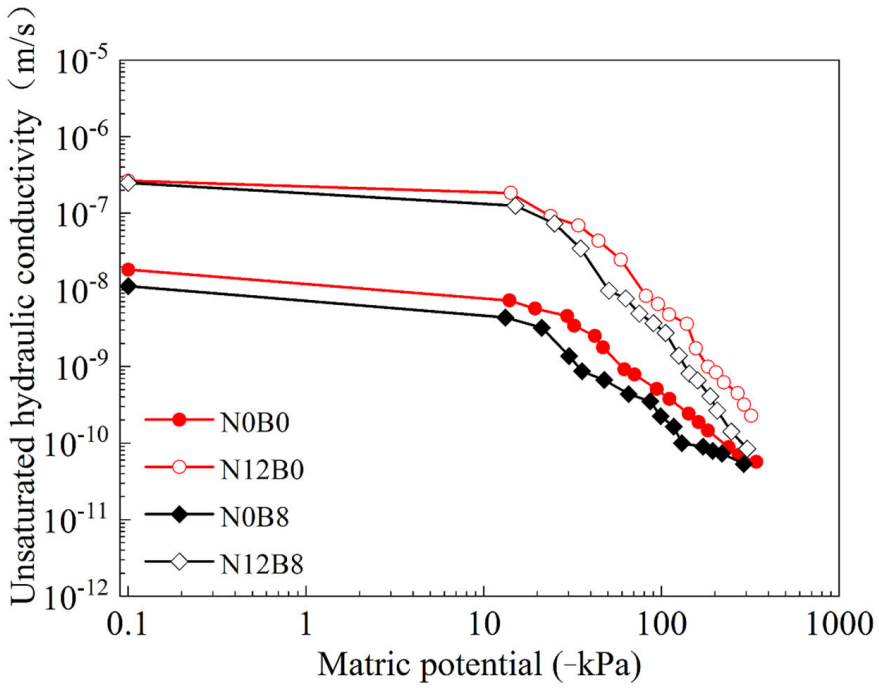


**Figure 7.** The effects of freezing–thawing on the unsaturated hydraulic conductivity of BAC with and without biochar treatment.

## 4. Conclusions

This study investigated the effects of freezing–thawing cycles on the unsaturated hydraulic properties of BAC. The unsaturated hydraulic properties were determined through a series of evaporation tests. The tests considered several factors that could potentially affect the properties, including biochar content and soil dry density. The conclusions from this study are summarised as follows: (i) The freezing–thawing process impacts clay's water retention and hydraulic conductivity by creating soil macropores and cracks, with the greatest increase in conductivity observed at high matric potentials. However, this effect diminishes when the matric potential drops below −30 kPa, leading to a lesser difference in conductivity. (ii) The addition of biochar counteracts the negative impacts of freeze–thaw cycles by transforming large pores into micro- or meso-pores, thereby reducing hydraulic conductivity, particularly effective at higher biochar concentrations. (iii) Although more

significant at high matric potentials, biochar still notably decreases conductivity at lower potentials. (iv) The soil total porosity increased with low application amounts (0% and 1%) but decreased with high application amounts (2% and 3%), with increasing numbers of freeze–thaw cycles. The characteristics of the soil freezing–thawing deformation changed from frost heaving to thaw settlement with increasing biochar application amounts, and an appropriate biochar application amount inhibited soil freezing–thawing deformation. The effects of soil and biochar types on the hydraulic properties of BAC under freeze–thaw environments may vary depending on the soil's pore distribution and the specific characteristics of the biochar used. This study highlights the value of BAC in enhancing soil properties under freeze–thaw conditions, which could improve soil stability and improve water retention in cold regions, emphasising the potential of biochar as a beneficial soil amendment in agriculture to counteract the effects of freezing and thawing.

**Author Contributions:** Conceptualization, Z.C.; Data curation, N.S.; Formal analysis, Z.C. and R.C.; Funding acquisition, V.K.; Investigation, Z.C., R.C. and V.K.; Methodology, Z.C., R.C. and V.K.; Visualisation, C.I. and N.S.; Writing—original draft, Z.C.; Writing—review and editing, V.K., R.C., C.I. and N.S. All authors have read and agreed to the published version of the manuscript.

**Funding:** This research was funded by the grant (RE-KRIS/FF67/003) from King Mongkut's Institute of Technology Ladkrabang (KMITL) and National Science, Research and Innovation Fund (NSRF).

**Data Availability Statement:** The original contributions presented in the study are included in the article, further inquiries can be directed to the corresponding author.

**Conflicts of Interest:** Author Zhongkui Chen was employed by the company Shenzhen Yanzhi Science and Technology Co., Ltd. The remaining authors declare that the research was conducted in the absence of any commercial or financial relationships that could be construed as a potential conflict of interest.

## References

1. Fu, Q.; Zhao, H.; Li, T.X.; Hou, R.J.; Liu, D.; Ji, Y.; Zhou, Z.Q.; Yang, L.Y. Effects of biochar addition on soil hydraulic properties before and after freezing-thawing. *Catena* **2019**, *176*, 112–124. [CrossRef]
2. Sahin, U.; Angin, I.; Kiziloglu, F.M. Effect of freezing and thawing processes on some physical properties of saline–sodic soils mixed with sewage sludge or fly ash. *Soil Tillage Res.* **2008**, *99*, 254–260. [CrossRef]
3. Xie, S.B.; Qu, J.J.; Lai, Y.M. Effects of freeze-thaw cycles on soil mechanical and physical properties in the Qinghai-Tibet Plateau. *J. Mt. Sci.* **2015**, *12*, 999–1099. [CrossRef]
4. Fouli, Y.; Cade-Menun, B.J.; Cutforth, H.W. Freeze-thaw cycles and soil water content effects on infiltration rate of three Saskatchewan soils. *Can. J. Soil Sci.* **2013**, *93*, 485–496. [CrossRef]
5. Cheng, Q.; Tang, C.S.; Xu, D.; Zeng, H.; Shi, B. Water infiltration in a cracked soil considering effect of drying-wetting cycles. *J. Hydrol.* **2020**, *593*, 125640. [CrossRef]
6. Yang, Z.N.; Lv, J.H.; Shi, W.; Jia, C.; Wang, C.; Hong, Y.; Ling, X.Z. Experimental study of the freeze thaw characteristics of expansive soil slope models with different initial moisture contents. *Sci. Rep.* **2021**, *11*, 23177. [CrossRef]
7. Liu, B.; Ma, R.M.; Fan, H.M. Evaluation of the impact of freeze-thaw cycles on pore structure characteristics of black soil using X-ray computed tomography. *Soil Tillage Res.* **2021**, *206*, 104810. [CrossRef]
8. Ma, R.; Jiang, Y.; Liu, B.; Fan, H. Effects of pore structure characterized by synchrotron-based micro-computed tomography on aggregate stability of black soil under freeze-thaw cycles. *Soil Tillage Res.* **2021**, *207*, 104855. [CrossRef]
9. Ng, C.W.W.; Li, Z.Y.; Zhang, Q.; Zhang, S.; Wang, Y.K. Effects of soil structure on cyclic freeze-thaw induced volumetric behaviour using a modified double-cell triaxial system. *Cold Reg. Sci. Technol.* **2022**, *203*, 103648. [CrossRef]
10. Apriyono, A.; Yuliana; Kamchoom, V. Serviceability of cut slope and embankment under seasonal climate variations. *Acta Geophys.* **2023**, *71*, 983–995. [CrossRef]
11. Liu, Y.Q.; Wang, X.C.; Wen, Y.J.; Cai, H.X.; Song, X.M.; Zhang, Z.P. Effects of freeze-thaw cycles on soil greenhouse gas emissions: A systematic review. *Environ. Res.* **2024**, *248*, 118386. [CrossRef] [PubMed]
12. Leuther, F.; Schlüter, S. Impact of freeze-thaw cycles on soil structure and soil hydraulic properties. *Soil* **2021**, *7*, 179–191. [CrossRef]
13. Qin, Y.; Bai, Y.F.; Chen, G.S.; Liang, Y.J.; Li, X.Y.; Wen, B.L.; Lu, X.R.; Li, X.J. The effects of soil freeze–thaw processes on water and salt migrations in the western Songnen Plain, China. *Sci. Rep.* **2021**, *11*, 3888. [CrossRef]

14. Apriyono, A.; Yuliana, Y.; Chen, Z.; Keawsawasvong, S.; Kamchoom, V. The impact of biochar amendment on soil water infiltration and evaporation under climate change scenarios. *Acta Geophys.* **2024**, *72*, 3647–3660. [CrossRef]
15. Chen, Z.; Kamchoom, V.; Chen, R.; Prasittisopin, L. Investigating the impacts of biochar amendment and soil compaction on unsaturated hydraulic properties of silty sand. *Agronomy* **2023**, *13*, 1845. [CrossRef]
16. He, X.L.; Yang, Y.R.; Huang, B.S.; Wang, Z.H.; Wang, M.X. An overview of characteristic factors of biochar as a soil improvement tool in rice growth—A review. *Environ. Res.* **2024**, *242*, 117794. [CrossRef]
17. Chen, Z.K.; Chen, C.W.; Kamchoom, V.; Chen, R. Gas permeability and water retention of a repacked silty sand amended with different particle size of peanut shell biochar. *Soil Sci. Soc. Am. J.* **2020**, *84*, 1630–1641. [CrossRef]
18. Garg, A.; Huang, H.; Cai, W.; Reddy, N.G.; Chen, P.; Han, Y.; Kamchoom, V.; Zhu, H.H. Influence of soil density on gas permeability and water retention in soils amended with in-house produced biochar. *J. Rock Mech. Geotech.* **2021**, *13*, 593–602. [CrossRef]
19. Chen, Z.K.; Kamchoom, V.; Apriyono, A.; Chen, R.; Chen, C.W. Laboratory study of water infiltration and evaporation in biochar-amended landfill covers under extreme climate. *Waste Manag.* **2022**, *153*, 323–334. [CrossRef]
20. Chen, Z.K.; Kamchoom, V.; Chen, R. Landfill gas emission through compacted clay considering effects of crack pathway and intensity. *Waste Manag.* **2022**, *143*, 215–222. [CrossRef]
21. He, Y.; Chen, X.; Peng, Y.; Luo, Z.B.; Jiang, S.F.; Jiang, H. Investigation of the effects of biochar amendment on soil under freeze–thaw cycles and the underlying mechanism. *Heliyon* **2024**, *10*, e34907. [CrossRef] [PubMed]
22. Chen, R.; Luo, Z.; Zhang, L.; Li, Z.; Tan, R. A new flexible-wall triaxial permeameter for localized characterizations of soil suffusion. *Q. J. Eng. Geol. Hydrogeol.* **2025**, *58*. [CrossRef]
23. Faloye, O.T.; Ajayi, A.E.; Kamchoom, V.; Akintola, O.A.; Oguntunde, P.G. Evaluating the impact of biochar and inorganic fertilizer applications on maize yield using multivariate statistical approach. *Agronomy* **2024**, *14*, 1761. [CrossRef]
24. Faloye, O.T.; Ajayi, A.E.; Oguntunde, P.G.; Kamchoom, V.; Fasina, A. Modeling and optimization of maize yield and water use efficiency under biochar, inorganic fertilizer and irrigation using principal component analysis. *Agriculture* **2024**, *14*, 1813. [CrossRef]
25. Jabro, J.D.; Iversen, W.M.; Evans, R.G.; Allen, B.L.; Stevens, W.B. Repeated freeze–thaw cycle effects on soil compaction in a clay loam in northeastern Montana. *Soil Sci. Soc. Am. J.* **2014**, *78*, 737–744. [CrossRef]
26. Hussain, R.; Ravi, K.; Garg, A. Influence of biochar on the soil water retention characteristics (SWRC): Potential application in geotechnical engineering structures. *Soil Tillage Res.* **2020**, *204*, 104713. [CrossRef]
27. Jeffery, S.; Meinders, M.B.J.; Stoof, C.R.; Bezemer, T.M.; van de Voorde, T.F.J.; Mommer, L.; van Groenigen, J.W. Biochar application does not improve the soil hydrological function of a sandy soil. *Geoderma* **2015**, *251–252*, 47–54. [CrossRef]
28. *GB/T 50123-2019*; Standard for Geotechnical Testing Method. China Planning Press: Beijing, China, 2019.
29. Ng, C.W.W.; Chen, Z.K.; Coo, J.L.; Chen, R.; Zhou, C. Gas breakthrough and emission through unsaturated compacted clay in landfill final cover. *Waste Manag.* **2015**, *44*, 155–163. [CrossRef]
30. *ASTM D6035/D6035M-13*; Standard Test Method for Determining the Effect of Freeze-Thaw on Hydraulic Conductivity of Compacted or Intact Soil Specimens Using a Flexible Wall Permeameter. American Society for Testing Materials: West Conshohocken, PA, USA, 2013.
31. *ASTM C1202*; Standard Test Method for Electrical Indication of Concrete's Ability to Resist Chloride Ion Penetration. American Society for Testing Materials: West Conshohocken, PA, USA, 2006.
32. Schindler, U.; Müller, L. Simplifying the evaporation method for quantifying soil hydraulic properties. *J. Plant Nutr. Soil Sci.* **2006**, *169*, 623–629. [CrossRef]
33. Chen, R.; Huang, J.W.; Chen, Z.K.; Xu, Y.; Liu, J.; Ge, Y.H. Effect of root density of wheat and okra on hydraulic properties of an unsaturated compacted loam. *Eur. J. Soil Sci.* **2019**, *70*, 493–506. [CrossRef]
34. Chen, R.; Liu, J.; Li, J.H.; Ng, C.W.W. An integrated high capacity tensiometer for measuring water retention curves continuously. *Soil Sci. Soc. Am. J.* **2015**, *79*, 943–947. [CrossRef]
35. van Genuchten, M.T. A closed-form equation for predicting the hydraulic conductivity of unsaturated soils. *Soil Sci. Soc. Am. J.* **1980**, *44*, 892–898. [CrossRef]
36. Sokolov, P.A.; Belousov, M.V.; Bondarev, S.A.; Zhouravleva, G.A.; Kasyanenko, N.A. FibrilJ: ImageJ plugin for fibrils' diameter and persistence length determination. *Comput. Phys. Commun.* **2017**, *214*, 199–206. [CrossRef]
37. Kumari, K.G.I.D.; Moldrup, P.; Paradelo, M.; Elsgaard, L.; de Jonge, L.W. Effects of biochar on dispersibility of colloids in agricultural soils. *J. Environ. Qual.* **2017**, *46*, 143–152. [CrossRef]
38. Jia, A.; Song, X.; Li, S.; Liu, Z.; Liu, X.; Han, Z.; Gao, H.; Gao, Q.; Zha, Y.; Liu, Y.; et al. Biochar enhances soil hydrological function by improving the pore structure of saline soil. *Agr. Water Manag.* **2024**, *306*, 109170. [CrossRef]
39. Yang, W.; Shang, J.Y.; Li, B.G.; Flury, M. Surface and colloid properties of biochar and implications for transport in porous media. *Crit. Rev. Environ. Sci. Technol.* **2019**, *50*, 2484–2522. [CrossRef]

40. Major, J.; Steiner, C.; Downie, A.; Lehmann, J. Biochar effects on nutrient leaching. In *Biochar for Environmental Management: Science and Technology*; Lehmann, J., Joseph, S., Eds.; Earthscan: London, UK, 2009; pp. 271–288.
41. Wong, J.T.F.; Chen, Z.K.; Wong, A.Y.Y.; Ng, C.W.W.; Wong, M.H. Effects of biochar on hydraulic conductivity of compacted kaolin clay. *Environ. Pollut.* **2018**, *234*, 468–472. [CrossRef]
42. Edeh, I.G.; Mašek, O.; Buss, W. A meta-analysis on biochar's effects on soil water properties—New insights and future research challenges. *Sci. Total Environ.* **2020**, *714*, 136857. [CrossRef]
43. Wang, T.; Li, P.; Ren, Z.P.; Xu, G.C.; Li, Z.B.; Yang, Y.Y.; Tang, S.S.; Yao, J.W. Effects of freeze-thaw on soil erosion processes and sediment selectivity under simulated rainfall. *J. Arid Land* **2017**, *9*, 234–243. [CrossRef]
44. Zhu, L.; Chen, N.; Zhang, X.; Ren, L.; Zou, R.; Xie, J.; Wang, Z.; Yang, H.; Hao, Z.; Qin, J.; et al. Freeze–thaw cycle events enable the deep disintegration of biochar: Release of dissolved black carbon and its structural-dependent carbon sequestration capacity. *Environ. Sci. Technol.* **2024**, *58*, 20979–20989. [CrossRef]
45. Liu, B.; Fan, H.M.; Jiang, Y.; Ma, R.M. Evaluation of soil macro-aggregate characteristics in response to soil macropore characteristics investigated by X-ray computed tomography under freeze-thaw effects. *Soil Tillage Res.* **2023**, *225*, 105599. [CrossRef]
46. Zhang, Z.; Ma, W.; Feng, W.J.; Xiao, D.H.; Hou, X. Reconstruction of soil particle composition during freeze-thaw cycling: A review. *Pedosphere* **2016**, *26*, 167–179. [CrossRef]
47. Li, Z.F.; Zhang, Y.F.; Chen, R.; Tai, P.; Zhang, Z.T. Numerical investigation of morphological effects on crushing characteristics of single calcareous sand particle by finite-discrete element method. *Powder Technol.* **2025**, 120592. [CrossRef]
48. Zuo, Y.T.; Meng, F.X.; Li, T.X.; Fu, Q.; Liu, D.; Hou, R.J.; Li, Q.L.; Li, M. Effect of biochar application on freezing-thawing deformation of farmland soil during freeze–thaw cycling. *Geoderma* **2022**, *405*, 115510. [CrossRef]
49. Zhang, T.; Che, A.L. A study on macro and micro characteristics and correlation of soil under cyclic freeze–thaws. *J. Mater. Civ. Eng.* **2022**, *34*, 04022232. [CrossRef]